Life Sciences 230 (2019) 178–187

Contents lists available at ScienceDirect

Life Sciences

journal homepage: www.elsevier.com/locate/lifescie

Bacterial membrane destabilization with cationic particles of nano-silver to combat efflux-mediated antibiotic resistance in Gram-negative bacteria

Samir A. Anuj[a,*], Harsukh P. Gajera[b], Darshna G. Hirpara[b], Baljibhai A. Golakiya[b]

[a] School of Science, RK University, Rajkot, Gujarat, India
[b] Department of Biotechnology, College of Agriculture, Junagadh Agricultural University, Junagadh, Gujarat, India

ARTICLE INFO

Keywords:
Linezolid
Efflux-mediated resistance
Nano-silver
Zeta potential
Membrane permeability

ABSTRACT

Aims: With the purpose of exploring combinatorial options that could enhance the bactericide efficacy of linezolid against Gram-negative bacteria, we assessed the extent of combination of nano-silver and linezolid.
Main methods: In this study, we selected *Escherichia coli* MTCC 443 as a model to study the combinatorial effect of nano-silver and linezolid to combat efflux-mediated resistance in Gram-negative bacteria. The acting mechanism of nano-silver on *E. coli* MTCC 443 was investigated by evaluating interaction of nano-silver with bacterial membrane as well as bacterial surface charge, morphology, intracellular leakages and biological activities of membrane bound respiratory chain dehydrogenase and deoxyribonucleic acids (DNA) of the cells following treatment with nano-silver.
Key findings: The alternation of zeta potential due to the interaction of nano-silver towards bacterial membrane proteins was correlated with enhancement of membrane permeability, which allows the penetration of linezolid into the cells. In addition, the binding affinity of nano-silver towards bacterial membrane depressed biological activities of membrane bound respiratory chain dehydrogenases and DNA integrity.
Significance: Our findings suggested that nano-silver could not only obstruct the activities of efflux pumps, but also altered membrane integrity at the same time and thus increased the cytoplasmic concentration of the linezolid to the effective level.

1. Introduction

Disease causing and antibiotic resistant bacteria are emerging pathogens whose resistance profiles create a major health crisis for containing their impact on human health. By the late 1970s, the problem of disease-causing, antibiotic-resistant bacteria emerged as nosocomial pathogens [1]. Among those, the increasing resistance in Gram-negative bacteria is concerning because they are becoming resistant to one or more of the antibiotics that would be considered for the treatment [2,3]. Recently, the public health officials reported a case of a Nevada woman who died from a Gram-negative *Klebsiella pneumonia* that was resistant to all available antibiotics in the United States, including tigecycline, a tetracycline derivative developed to control emerging antibiotic resistance [4]. Although bacterial resistance to different antibiotics occurs normally because of antibiotic target alternation, enzymatic inactivation of antibiotics, decrease in the antibiotic uptake and lack of pro-antibiotic activation due to increased efflux [5]. In Gram-negative bacteria, efflux of the antibiotics is concerning especially because multidrug efflux pumps of carbapenem-resistant Enterobacteriaceae (CRE) can develop a simultaneous resistance to different antibiotics [6]. Efflux pumps are membrane-bound transporter proteins involved in drug exclusion from within bacterial cells into the surrounding environment [7]. In an increasing number of multidrug-resistant cases, patients have to be treated with older alternatives such as silver and silver based compounds. However, chronic intake of silver has been implicated in a variety of conditions, argyria being the best known [8].

Nanotechnology offers opportunities to re-explore the biochemical properties of already known bactericide compounds at atomic and molecular level to minimize their cytotoxic effect. Silver in different chemical forms has high toxicity; nano-silver has gained more attention nowadays [9]. In addition, it was found that nano-silver had

Abbreviations: CRE, carbapenem-resistant Enterobacteriaceae; MRSA, Methicillin-resistant *Staphylococcus aureus*; IMTECH, Institute of Microbial Technology; MTCC, Microbial Type Culture Collection; DLS, Dynamic Light Scattering; SEM, Scanning Electron Microscopy; EDX, Energy Dispersive Spectroscopy; ZnO, zinc oxide; GC–MS, Gas Chromatography- Mass Spectrometry; PDI, Polydispersity Index; NIST, National Institute Standard and Technology

* Corresponding author at: School of Science, RK University, Bhavnagar Highway, Kasturbadham, Rajkot 360020, Gujarat, India.
E-mail address: samiranuj@gmail.com (S.A. Anuj).

https://doi.org/10.1016/j.lfs.2019.05.072
Received 17 April 2019; Received in revised form 22 May 2019; Accepted 27 May 2019
Available online 29 May 2019

bactericidal property against multidrug-resistant bacteria [10–12]. However, the exact mode of actions of nano-silver is unknown, but now it is well established that nano-silver accumulate at membrane of bacteria leading to their destabilization [13].

Another category of bactericide, a synthetic bacteriostatic antibiotic linezolid (Zyvox), belongs to the oxazolidinones class of antibiotics. Oxazolidinones are active mainly against Gram-positive cocci, some Gram-negative anaerobes, *Nocardia* species and mycobacteria species [14]. It inhibits bacterial growth by inhibiting the initiation process at a very earlier stage in protein synthesis [15]. However, oxazolidinones generally are not active against aerobic Gram-negative organisms such as *E. coli* due to rapid efflux mechanisms [16]. To resolve the problem of rapid efflux of linezolid, both nano-silver and linezolid must be used to be effective along with each other, and also these bactericides be utilized together. The fact is that nano-silver engaged in surface disruption and linezolid caused protein synthesis inhibition. Such combination of linezolid and nano-silver blocked the defined bacterial mechanism of resistance, which cause bacteria to die eventually.

Present study aimed to understand the acting mechanism of nano-silver and established the mechanism of inhibition to *E. coli* MTCC 443 through destroying membranous structure in the presence of linezolid. The purpose of study was also to investigate how linezolid prevent the growth of Gram-negative bacteria and even kill the cells regardless of their rapid efflux mechanisms along with nano-silver. For the first time, we offer evidences to indicate that linezolid and nano-silver worked synergistically on Gram-negative bacteria, and provided an idea towards the extent to which the efficacy of linezolid as bactericidal agents would be advantaged in the presence of representative nano-silver.

2. Materials and methods

2.1. Materials

The stems of *Tinospora cordifolia* (Gir forest, Gujarat, India) was collected based on its medicinal property [17]. Linezolid (Sigma Aldrich, Bengaluru, India) dissolved in Milli-Q water to final concentration 100 μg/mL. The bacterial strains *E. coli* MTCC 443 and *Staphylococcus aureus* MTCC 3160 (IMTECH, Chandigarh, India) belong to multiple drug resistant clinical isolate were used for the bactericidal assessment [18,19]. Aqueous solution (10^{-3} M) of Silver nitrate (Thermo Fisher Scientific, Telangana, India) was prepared in Milli-Q water.

2.2. Preparation of the stem extract from T. cordifolia

The stem of *T. cordifolia* taken and dried under ambient temperature (37 °C) followed by ground into a fine powder. About 5 g of powder along with 100 mL of Milli-Q water was boiled at 70 °C for 10 min. in a 250 mL Erlenmeyer flask. The extract was then filtered twice through Whatman No. 1 filter paper to get clear solution, which was then refrigerated, at 4 °C for further experiments [20].

2.3. Green synthesis and characterization of nano-silver

To synthesize small and stable nano-silver particles with positive charge, the previous synthesized method described by Anuj SA et al. was carried out using stem extract of *T. cordifolia* with 10^{-3} M silver nitrate concentration in light condition at 40 °C [20]. After 12 h, the colour of the solution changed from light yellow to yellowish brown and finally dark brown, indicating the formation of nano-silver particles. At first, nano-silver was characterized by scanning the absorbance spectra in 300–700 nm range of wavelength by UV–Visible spectrophotometer (Agilent Technologies, Cary 60). Further confirmation of the average size and zeta potential of synthesized nano-silver was determined by dynamic Nanotrac Wave (Model S3500) based on Dynamic Light Scattering (DLS). Finally, Scanning Electron Microscopy (Ziss, EVO-18) with an Energy Dispersive X-Ray (EDX) facility was used to determine the size and composition of the nano-silver.

2.4. Study of predicting nano-silver interaction with protein targets

The chemical-protein interaction network analysis was used to predict the action of nano-silver against efflux-mediated resistance. Targeted efflux transport proteins of *E. coli* 536 were identified based on STITCH 5.0, a pre-computed database resource that includes many experimental sources with text-mining prediction and evidences [21]. In STITCH 5.0 database, there are no any information available for *E. coli* MTCC 443 strain; hence, we used *E. coli* 536 for interaction study. This database offers several short tutorial to introduce the different query options such as searching for a single identifier or multiple biochemical configurations. In 2016, Szklarczyk D et al. released 5th version of STITCH, which contains chemical-protein interactions for between 300,000 small molecules and 2.6 million proteins from 1133 organisms [22]. The STITCH database provides a confidence measure for each chemical-protein interaction through score equation 1- πi (1-*p*i), where *p*i denotes the confidence of the chemical-protein interaction from the i^{th} information source [23]. Based on STITCH score equation, a score between 0.40 and 0.70 indicates medium, between 0.7 and 0.90 indicates high and between 0.90 and 1.00 indicates the highest confidence. Along with STITCH 5.0, several other databases such as Gene Ontology (GO), Protein Data Bank (PDB), Kyoto Encyclopedia of Genes and Genomes (KEGG), DrugBank, and Reactome, offer valuable information regarding functional partners and annotations [24–26]. The STITCH 5.0 database also provided the interactions between linezolid and proteins to understand the mode of action of linezolid.

2.5. Surface potential neutralization of E. coli MTCC 443 by nano-silver

Bactericidal activity of nano-silver was characterized by alternation in their membrane depolarization, which allows the measurement of zeta potential of bacteria. In the experiment, bacterial cells (10^8 CFU/mL) treated with 100 μg/mL of nano-silver were harvested by centrifugation (1000 rpm for 10 min), and the cells washed twice with potassium phosphate buffer solution (pH 7.2) to avoid any influence of pH and finally re-suspended in the same buffer [27]. Zeta potential measured with Nanotrac Wave (S3500) along with different time intervals (up to 8 h) for a better understanding of the action of nano-silver. Zeta potential also carried out for autoclaved (at 120 °C, 15 psi for 20 min) bacterial cells. Each of the experiments was conducted in triplicate under identical condition.

2.6. Effect of nano-silver on the morphology of E. coli MTCC 443

The morphological changes of bacterial cells treated or not with nano-silver were observed under SEM, particularly initial interaction of nano-silver towards bacterial cells. Bacterial cells (10^8 CFU/mL) treated with 100 μg/mL of nano-silver were collected (1000 rpm for 10 min) after 3 h washed twice and re-suspended in PBS. The bacterial cells were fixed with 2.5% glutaraldehyde for 2 h at room temperature, dehydrated with a series of ethanol solutions (30, 50, 70, 80 and 90%). The fixed cell was dried at 37 °C in sterile conditions and examined using SEM (Zeiss, Model EVO-18). EDX was also performed to visualize the morphological interaction between nano-silver and bacterial cells [28].

2.7. Gas Chromatography- Mass Spectrometry (GC–MS) analysis for leakages of intracellular constituents from E. coli MTCC 443

GC–MS analysis was carried out for identifying the leakages of intracellular constituents from bacterial cells (10^8 CFU/mL) treated or non-treated with nano-silver (100 μg/mL).

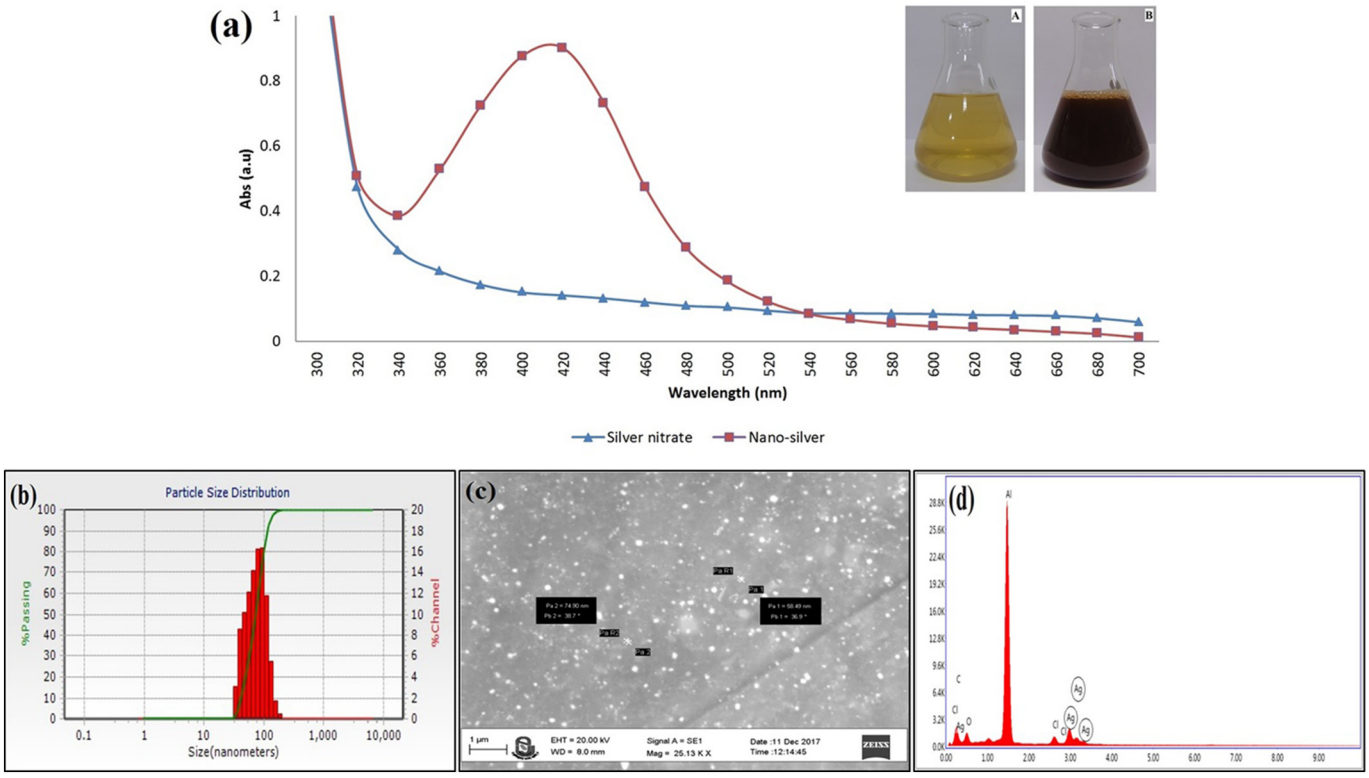

Fig. 1. Characterization of green synthesized nano-silver. (a) UV–Visible spectra and figure inset shows the colour changes before-A and after-B synthesis of nano-silver. (b) Histogram of particle size distribution by dynamic light scattering, (c) SEM micrographs and (d) EDX spectrum. (For interpretation of the references to colour in this figure legend, the reader is referred to the web version of this article.)

2.7.1. Derivatization

Bacterial cell extract (water 100 v/v) was dried at 40 °C in Nitrogen Turbo Evaporator (Biotage, TurboVap®LV). Dried cell extract was derivatized with 80 µL of a 20 mg/mL methoxyamine hydrochloride solution in 1 mL of pyridine for 90 min at 37 °C on shaker. Subsequently, the samples were silylated for 60 min at 37 °C with 160 µL N,O-Bis (trimethylsilyl) trifluoroacetamide (BSTFA) on shaker.

2.7.2. Condition for GC–MS profiling

The derivatized extract was analyzed with Gas Chromatograph-Mass Spectrometer (GCMS-QP2010 Plus, Shimadzu, Japan) coupled with Shimadzu GCMS-QP2010 SE mass selective detector. 1 µL aliquots of the extracts were injected into a DB-17 MS capillary column (60 m × 0.25 mm I.D., 0.25 µm film thickness) using splitless injection (230 °C, 1.5 min). Helium was used as a carrier gas at a flow rate of 1 mL/min.

2.7.3. Peak identification of intracellular leakages

Compounds were identified by mass spectra analysis (50–700 *m/z* range) through the National Institute Standard and Technology (NIST) library 2012 and GC–MS solution software to calculate the similarity index. Relative area (%) of each unknown compound was calculated by the ratio between the compound peak area and the sum of all peak areas of unknown compounds. The mass spectrum of identified compound was compared with the spectrum of the known compounds stored in the NIST library. A similarity index above 90% was considered acceptable [20,29].

2.8. Effect of nano-silver on membrane bound enzyme and genomic DNA

The following assays were performed to observe the obstructive effect of nano-silver on membrane bound respiratory chain dehydrogenases and genomic DNA of non-treated and treated cells.

2.8.1. Respiratory chain dehydrogenases activity of E. coli MTCC 443 influenced by nano-silver

The respiratory chain dehydrogenases activity was measured by assessing the reduction of colorless iodonitrotetrazolium chloride (INT) to a red iodonitrotetrazolium formazan (INF) [30]. Nano-silver (100 µg/mL) treated bacterial cells (10^8 CFU/mL) were incubated at 37 °C for 3 h in shaking condition. After this, the culture was collected (1000 rpm for 10 min), washed by phosphate buffer saline (PBS) and then suspended in 0.9 mL of PBS. Suspended culture was added into 0.1 mL, 0.5% INT solution and again incubated (37 °C for 2 h) in dark condition and then terminated the reaction by 100 µL formaldehyde.

2.8.2. Integrity of genomic DNA of E. coli MTCC 443 influenced by nano-silver

To determine whether nano-silver (100 µg/mL) has an effect on the DNA integrity of treated bacterial cells (10^8 CFU/mL), the amount of DNA from non-treated and nano-silver treated bacterial cells was extracted as per the manufactures guideline using a commercially available DNA extraction kit (Bangalore Genei, ™ India). The extracted bacterial DNA was subjected to agarose gel electrophoresis and visualized under Gel doc for integrity of DNA band [31].

2.9. Synergistic effect of nano-silver combined with linezolid on E. coli MTCC 443

The susceptibility of the bacterial cells to linezolid alone and in combination with nano-silver was determined by agar well diffusion assay with inoculations of 10^8 CFU/mL of *E. coli* MTCC 443. The Gram-positive *S. aureus* MTCC 3160 which is susceptible to linezolid also taken as positive control to check the synergistic effect of nano-silver and linezolid on said Gram-negative bacteria. The final concentration of linezolid, nano-silver and linezolid with nano-silver were adjusted to 10 µg/100 µL. Bacterial growth was observed after 24 h [13]. The assay

was performed in triplicate and standard deviation was calculated to test the level of significance.

3. Results and discussion

3.1. Characterization of green synthesized nano-silver

After synthesis of nano-silver particles, precise nanoparticle characterization is required, because the physiochemical properties of synthesized nanoparticles could have a significant effect on their biological properties. In our study, the resultant nano-silver suspension gave brown colour with a sharp surface Plasmon band at 418 nm, which is an expected characteristic of nano-silver (Fig. 1a). DLS technique has been used to determine the average size of nano-silver in the colloidal solution. The size of synthesized nano-silver was ranging from 41.80 to 129.40 nm, and the average size was found to be 73.90 nm as observed under DLS (Fig. 1b). The zeta potential value was found to +34.4. The cationic surface charge of zeta potential confirms the electrostatic repulsion among the nano-silver and thereby prevents the nano-silver from agglomeration in the suspension leading to long-term stability, as well as to increase their bactericidal efficiency through anionic biomolecules of bacterial cell membrane [32]. The SEM results showed that green synthesized nano-silver was spherical in shape with an average 66.70 nm size and found to be well dispersed in aqueous solution (Fig. 1c). The EDX revealed a strong signal in the silver region around 3 kV correspond to the binding energies of AgL with traces of O_K, Na_K, and N_K, which may be present in phytochemicals that are bound to the surface of nano-silver (Fig. 1d).

3.2. Study for predicting interactions between nano-silver and proteins

The chemical-protein binding information obtained from the STITCH 5.0 database was used to predict the interaction between nano-silver and bacterial proteins, which may obstructs the activity of proteins. Here, the main interactors of *E. coli* 536, which can interacts with nano-silver shown in Fig. 2(a). Majority of the interactors present in *E. coli* 536 are membranous proteins or enzymes that involved in the extrusion of toxic substances from the cells. The known main cusCBA efflux transport proteins complex is connected by very high confidence score (≥ 0.831) than other cytoplasmic proteins (Table S1). In *E. coli*, the cusCFBA complex is an important resistance nodulation cell division (RND) transporter with a specificity for heavy metals homeostasis. CusF, part of a cation efflux system, is expected to serve a metal-dependent regulatory function in its interactions with cusCBA complex, also interact (score: 0.817) with nano-silver [33]. The multi-copper oxidase cueO interact with nano-silver, which are require for copper homeostasis in *E. coli* 536. Copper efflux regulator cueR regulates the transcription of the copA, which encodes a copper ATPase, and cueO, which encodes a copper oxidase. It detects copper stress and activates transcription of the copA and cueO in response to increasing cytoplasmic copper concentration [34]. Nano-silver also interact with cueR and stop the transcription activity in *E. coli* [35]. Nano-silver also binds with glutathione reductase (Gor), which is a flavoprotein that maintains high levels of reduced glutathione in the cytosol [35]. Binding to sthA gene with nano-silver may result the interruption in conversion of NADPH to NADH, which can enter the respiratory system for energy production [36]. Pyridine nucleotide-disulfide oxidoreductase is regulates by ykgC and ECP_4276 genes and involved in reactive chlorine species (RCS) stress resistance. Nano-silver interact with this gene and ultimately obstruct the activities of pyridine nucleotide-disulfide oxidoreductase. Previous STITCH 4.0 database studies on *E. coli* also showed that nano-silver interact with efflux system membranous proteins complex cusCBA and obstruct the membrane activity of bacteria [37].

Moreover, the STITCH 5.0 database provided the interactions between linezolid and bacterial proteins to find out the binding site of linezolid. Fig. 2(b) showed that linezolid strongly interacts (0.768 0.69) with 50S ribosomal proteins in *E. coli* 536 [38]. The confidence score of these interactors was from 0.690 to 0.768. In addition, linezolid also interact with acrB (acriflavine resistance protein B, score: 0.830), a subunit of multidrug efflux protein complex (AcrA-AcrB-AcrZ-TolC) with broad substance specificity that uses the proton motive force to export substances [39].

These interactions studies revealed that nano-silver strongly interacts with membrane bound efflux system proteins in *E. coli*. Interestingly, these findings confirmed that linezolid can interact with ribosomal proteins in *E. coli* and inhibits the protein synthesis in Gram-negative bacteria, if linezolid remain in the cells.

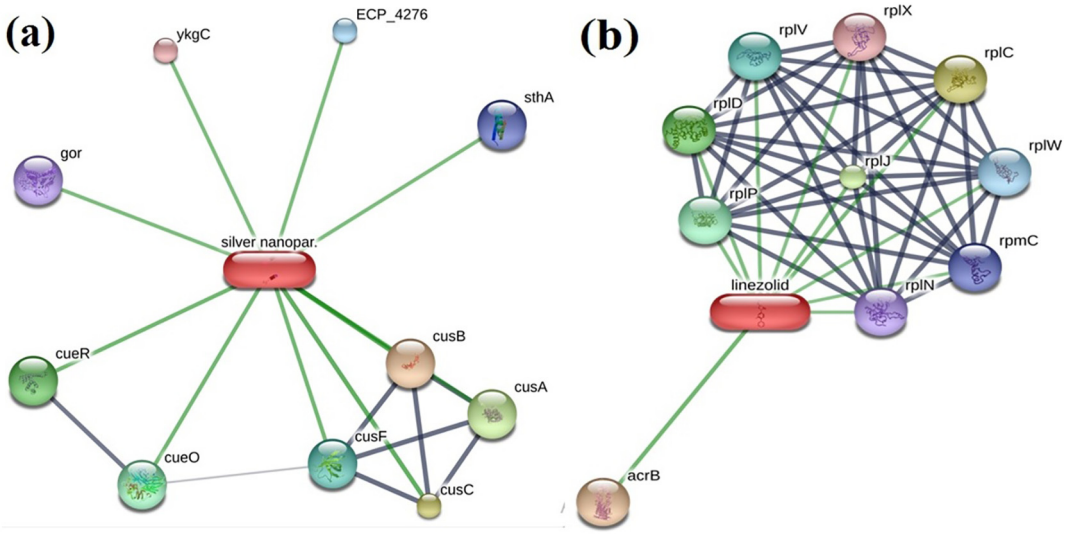

Fig. 2. Chemical-bacterial protein interaction networks based on STITCH 5.0 databases (a). Nano silver-protein interaction network and (b). Linezolid-protein interaction network of *E. coli* MTCC 443.
An individual line between protein and nano-silver or linezolid represents an interaction wherein thicker line for stronger association, green line for chemical- protein interaction and grey line for protein-protein interaction. (For interpretation of the references to colour in this figure legend, the reader is referred to the web version of this article.)

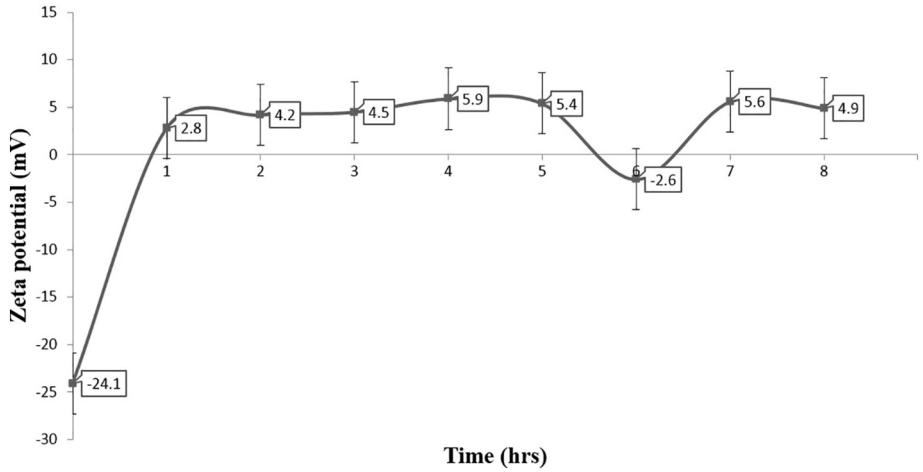

Fig. 3. Change in bacterial Zeta potential in presence of nano-silver. Each data point represents mean ± SD for three independent experiments.

3.3. Surface potential neutralization of *E. coli* MTCC 443 cells by nano-silver

Anionic bacterial membranes are important for the antibacterial activity of the certain cationic antibacterial substances, which acts on bacterial surface. The difference in zeta potential among different time intervals of bacterial cells suggested that membrane depolarization may affect the functioning of the cells, which cause bacteria to die eventually (Fig. 3). However, it may be pertinent to say that alternation in bacterial membrane depolarization may not always lead to bacterial cell death, rather depending on the magnitude of altered depolarization; the membrane integrity of the cell may be affected. In our study, the average Zeta potential of the normal and autoclaved *E. coli* MTCC 443 cells were found to be −24.1 and +2.2 mV, respectively (Data not shown in Fig. 3). There were significant differences in the zeta potentials of normal compared to treated cells, when they were exposed to nano-silver, at different time intervals (up to 8 h). In addition, it was also found that the magnitude of decrease in the negativity of the zeta potential was found to be maximum at the beginning of the treatment. Such alternation of zeta potential in *E. coli* MTCC 443 may be caused due to interaction between the higher amount of anionic compounds in lipopolysaccharides (LPS) membrane and cationic nano-silver. In Table 1, we have depicted the relationship between cell membrane disruption (measured by *Z*-average value) and polydispersity index (PDI) of the bacterial suspension, following exposure to nano-silver. The breaking of the cell significantly increased the bacterial size with increased PDI, as was noted in our finding. Similar results were also found when bacterial cells were treated with nanoparticles of ZnO, where cationic nanoparticles of ZnO were found to interact with anionic bacterial cell membrane and the overall zeta potential shifted towards neutrality [40]. Moreover, such alternation in zeta potential can be correlated with the increased intracellular constituents as was evident from GC–MS analysis (Fig. S1) [13,41]. Cationic nano-silver is known to interact with anionic bacterial outer surface, leading to damage of cell membrane structure, thus increasing leakage of bacterial intracellular constituents [20].

Table 1
The polydispersity index (measured by DLS) and damage of cells (expressed as cell size) after treatment with and without nano-silver.

Treatment	*Z*-average (μm)	PDI
Normal cell	1.12 ± 0.1200	0.26 ± 0.0018
Nano-silver treated cell	1.43 ± 0.2400	2.56 ± 0.1800
Heat treated cell	4.22 ± 0.5200	6.18 ± 0.3400

Values are expressed as mean ± SD; (n = 3).

3.4. Observation of the action of nano-silver on the morphology of *E. coli* MTCC 443

To find out how nano-silver affects the bacteria, SEM was used to illustrate interactions between nano-silver and *E. coli* MTCC 443 cells. The examination under SEM revealed that the surface of non-treated *E. coli* MTCC 443 cells were smooth, intact and showed typical characters of rod shape with 1.25 μm dimensions (Fig. 4a), however membrane of treated cells were damage severely (Fig. 4b). Another change induced by the nano-silver was the widening of the cell (1.93 μm) with large leakages (Fig. 4c). Similar morphological changes in *E. coli* cells have been observed in previous studies [42]. In addition, the interaction between nano-silver and the bacterial cell surface was proved by their aggregation on the cell surface and the formation of leakage sites (Fig. 4b), thus determining an enhanced permeability of the bacterial membrane which allowed entry of linezolid into the cell and caused its death. Exposure of the bacterial cells to the nano-silver causes rupture in the cell surface that may lead to cell death, as evident from significant increased the total intracellular constituents of the cell suspension against non-treated bacterial culture (Fig. S1).

3.5. GC–MS analysis for determination of intracellular constituents from *E. coli* MTCC 443

The leakage of intracellular constituents by nano-silver was confirmed by GC–MS analysis. In this study, almost no intracellular constituents could be detected to leak from non-treated cells, while the leakage of intracellular constituents was found from the treated cells (Fig. S1). After treatment with nano-silver for 3 h, the leakage amount of the intracellular constituents was elevated, suggesting that nano-silver was able to enhance the leakage of the intracellular constituents from bacteria. In the present finding, GC–MS analyses of the metabolites from treated bacteria identified around 92 resolved peaks. Among this, some components were from stem extract of *T. cordifolia*, by which we have synthesized nano-silver. GC–MS chromatogram showed that major metabolites in the treated bacterial cells are sugars, organic acids, amino acids and fatty acids, which showed significant differences in normal and treated cells (Table S2). Moreover, the common and unique compounds identified from *E. coli* MTCC 443 cells, before and after treatment with nano-silver along with plant extract are shown in Fig. 5a. Total 44 components were identified common to treat and plant extract followed by unique 23 compounds in treated cells and 13 in plant extract. In addition, only one compound found to be common for non-treated, treated and plant extract. An increase in unique compounds such as amino acids, polyamines and organic acids found in treated cells than non-treated cells confirmed bacterial membrane

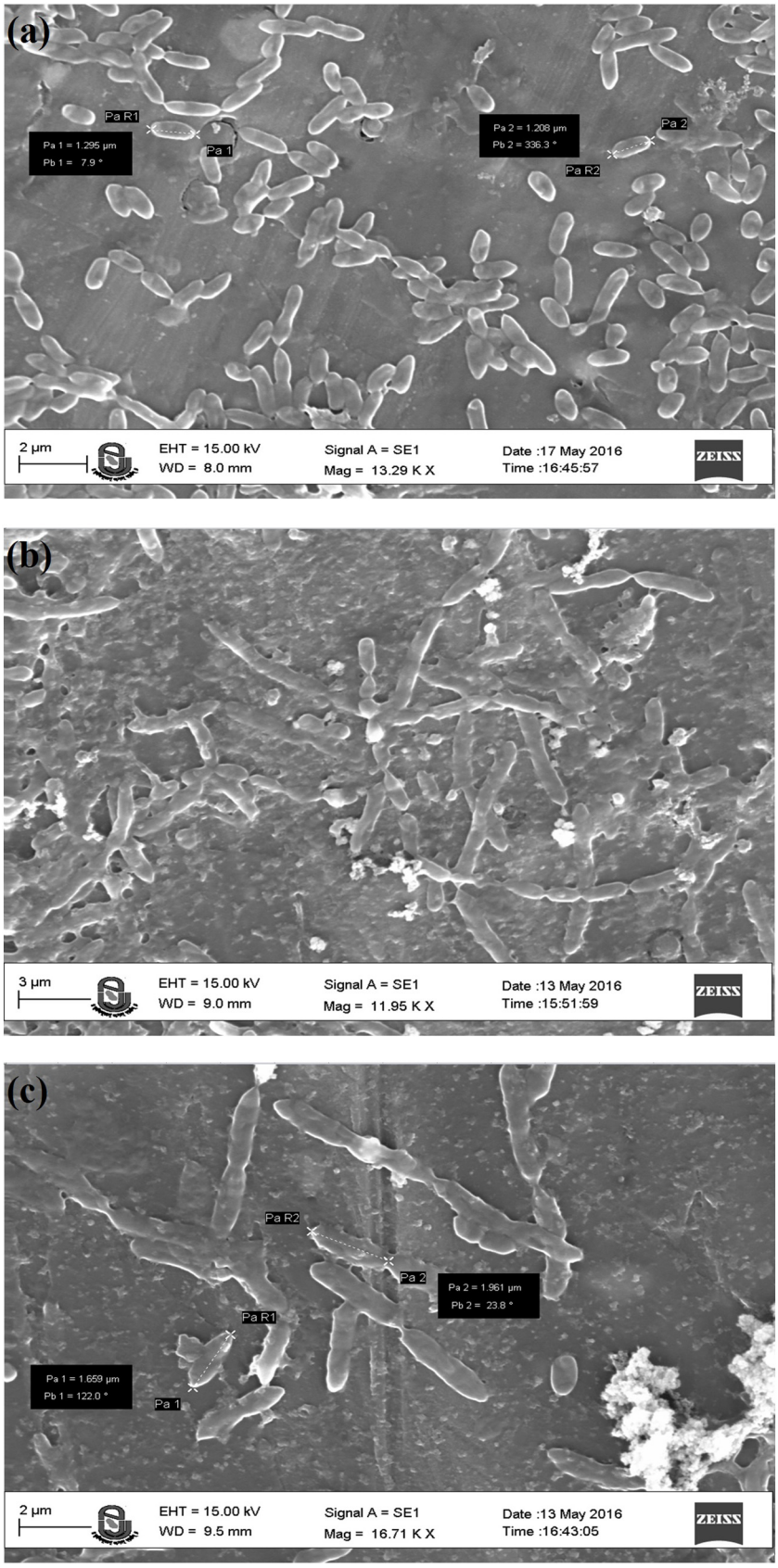

Fig. 4. SEM images depicting morphology of *E. coli* MTCC 443 cells influenced by nano-silver. (a). Structure of native cells, (b). Nano-silver interaction with bacterial cells and (c). Nano-silver treated damaged bacterial cells.

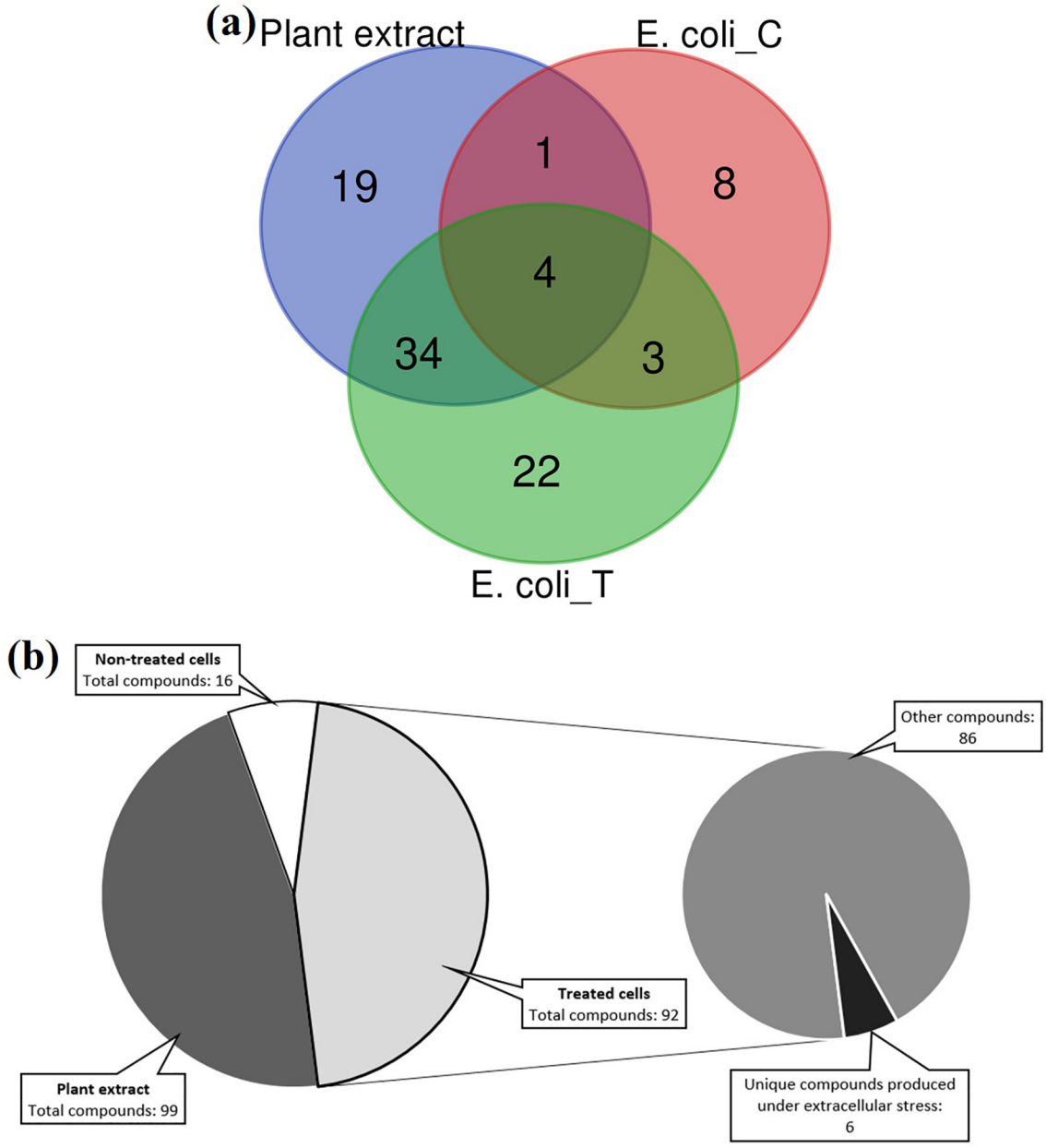

Fig. 5. (a). Venn diagram showing numbers of identified compounds from non-treated and nano-silver treated *E. coli* MTCC 443 cells as well as plant extract and (b). Unique compounds produced by *E. coli* MTCC 443 cells in response to extracellular stress.
Abbreviations: *E. coli*_C: Non-treated cells, *E. coli*_T: Treated cells.

destroying efficiency of nano-silver (Table S2). Anuj SA et al. found similar results in case of *Pseudomonas aeruginosa* and *Bacillus megaterium*, when the bacterial cells were treated with nano-silver [20].

Surprisingly, GC–MS analysis also confirmed response mechanism of *E. coli* MTCC 443 against nano-silver (Fig. 5b). In response to nano-silver, *E. coli* MTCC 443 secrete cadaverine, a polyamine known to inhibit porin mediated outer membrane permeability [43]. Furthermore, *E. coli* MTCC 443 also secrete various L-amino acids, which act as osmolytes and thus enable bacteria to survive under stress of nano-silver (Table 2) [44]. There have been no previous studies on leakages of intracellular constituents through nano-silver based on GC–MS analysis. GC–MS analysis confirmed that nano-silver has ability to altered bacterial membrane permeability.

Table 2
Compounds produced by *E. coli* MTCC 443 in response to nano-silver (identified by GC–MS spectra).

Class	Compounds	RT (min)	Peak area %	Peak no.
Amino acids	L-ornithine	0.34	19.512	30
	L-aspartic acid	0.55	13.144	11
	L-proline	0.79	17.264	23
	L-threonine	0.99	9.321	2
	L-methionine	1.64	14.766	15
Polyamine	Cadaverine	1.53	22.011	39

3.6. Assaying the effect of nano-silver on membrane bound enzyme and genomic DNA

To determine whether interaction between nano-silver and bacterial

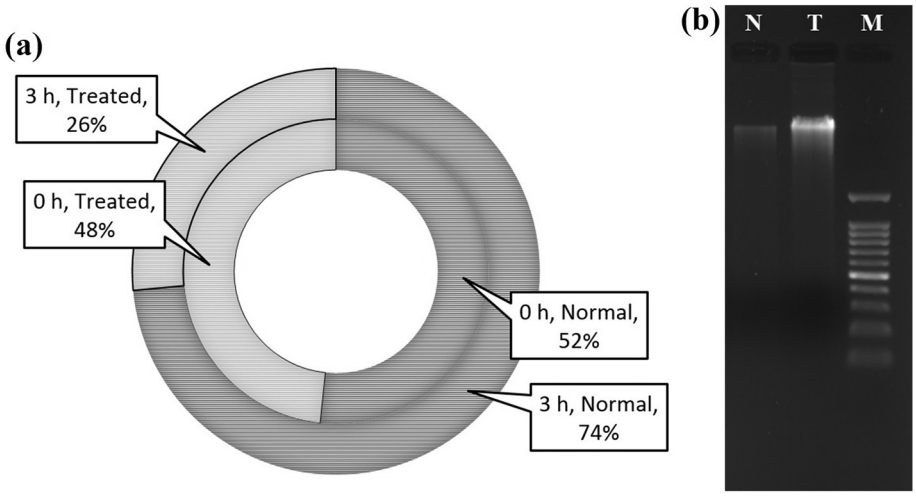

Fig. 6. Effect of nano-silver on membrane bound (a). Respiratory chain dehydrogenase and (b). DNA of *E. coli* MTCC 443. Abbreviations: N: Normal *E. coli* MTCC 443, T: Treated *E. coli* MTCC 443, M: Marker.

interface has an effect on the membrane bound enzymes or genomic DNA, the activity of respiratory chain dehydrogenase and decomposability of genomic DNA from non-treated and nano-silver treated cells measured, respectively.

3.6.1. Respiratory chain dehydrogenases activity of E. coli MTCC 443 influenced by nano-silver

The dehydrogenase activity of bacterial cells treated with nano-silver indicated that membrane destabilization by nano-silver associated with depression of the activity of dehydrogenase enzyme (Fig. 6a). Moreover, our findings showed that the initial dehydrogenase activity of treated cells was higher than that of incubated cells indicated that nano-silver could not only obstructs the activity of dehydrogenase but bacterial reproduction also. However, in case of non-treated cells, the dehydrogenase activity increased after 3 h compared to treated cells. Previously, Anuj SA et al. studied respiration-destroying efficacy of nano-silver in *S. aureus* MTCC 3160 by determining dehydrogenase activity involved in respiration. In 2011, Kim S et al. suggested that positively charged nano-silver interacted with –SH (thiol) group of cysteine and form –S–Ag, thus obstructing the dehydrogenase activity of nano-silver treated enzyme to prevent growth of bacteria [45]. However, the exact mechanism by which nano-silver destroyed the activity of enzymes still not completely understood.

3.6.2. Integrity of genomic DNA of E. coli MTCC 443 influenced by nano-silver

From our experimental data, we observed that the interaction of nano-silver with bacterial cells increased the decomposability of bacterial genomic DNA compared to non-treated cells (Fig. 6b). The decomposability of DNA may be due to the bacterial membrane interruption by nano-silver, which leads to disturbed membrane bound genomic DNA. Based on this finding, it can be suggested that altered membrane integrity may be disturbed intact organization of genomic DNA and therefore fuzzy band was observed in treated cells compared to non-treated cells where intact DNA was found. Hence, it is reasonable to conclude that the decomposability of bacterial genomic DNA observed in treated cells is due to their altered membrane integrity. Moreover, previous studies also revealed that the attachment of bacterial genomic DNA towards cell membrane is essential for DNA replication [46]. Based on these findings, we can also concluded that the bacterial membrane interruption may loss of DNA replication, which cause bacteria to die eventually. In a previous study, similar findings observed by Chen M et al. when bacterial cells treated with nano-silver [31]. In addition, the genes encoding for efflux transport proteins may be located on genomic DNA; hence, the decomposability of genomic DNA affect the transport activity of efflux pumps also [47].

3.7. Synergistic effect of nano-silver combined with linezolid on E. coli MTCC 443

The diseases that associated to membrane-bound efflux pumps lead to the emergence or re-emergence of antibiotic-resistant bacteria; due to this, silver in the nano form in combination with linezolid have been suggested as an alternative route to control emerging and re-emerging infectious diseases. When tested together, the two bactericides linezolid and nano-silver worked in an effective manner and showed synergistic effect for *E. coli* MTCC 443 (Fig. 7a). Linezolid alone showed relapse growth, whereas its combination with nano-silver prevented the emergence of *E. coli* MTCC 443. In case of nano-silver, compared to the effects of nano-silver alone, the combined effect of both them was more pronounced, which suggests synergistic activity of the two components. Hence, the membrane destroying property of nano-silver was taken up in combination with linezolid to increase its efficacy against Gram-negative *E. coli* MTCC 443 (Fig. 7a). The zones of inhibition of linezolid with and without nano-silver against test strains were presented in Table 3. It was clear that the combination was highly effective against the Gram-negative bacteria. The synergistic bactericide effect is likely due to hindrance in protein synthesis through linezolid assisted by nano-silver. This study demonstrates the synergistic action of nano-silver and linezolid to improve their bactericidal efficiency; it was suggested that linezolid could be used in combination with nano-silver in order to improve their bactericidal property against Gram-negative bacterial species. On the other hand, the synergistic action of linezolid alone and in combination with nano-silver was also investigated against Gram-positive *S. aureus* MTCC 3160 as positive control (Fig. 7b). When tested alone, linezolid was most effective against Gram-positive, whereas nano-silver showed slightly low activity compared to linezolid. There have been no previous studies on synergistic effect of nano-silver with linezolid to overcome efflux-mediated resistance issues. Moreover, our findings also suggested that Gram-positive *S. aureus* MTCC 3160 was more susceptible towards nano-silver than Gram-negative *E. coli* MTCC 443. Now, it is well established that Gram-positive bacteria lack outer membrane outside the peptidoglycan layer possessing in Gram-negative bacteria, which protects bacteria from toxic substances [48]. In addition, no any synergistic action was observed in case of *S. aureus* MTCC 3160 (Fig. 7b and Table 3). In combination, disrupted membrane may slightly prevent penetration of linezolid to the cell, and thus synergistic action was not observed. However, this study revealed a new

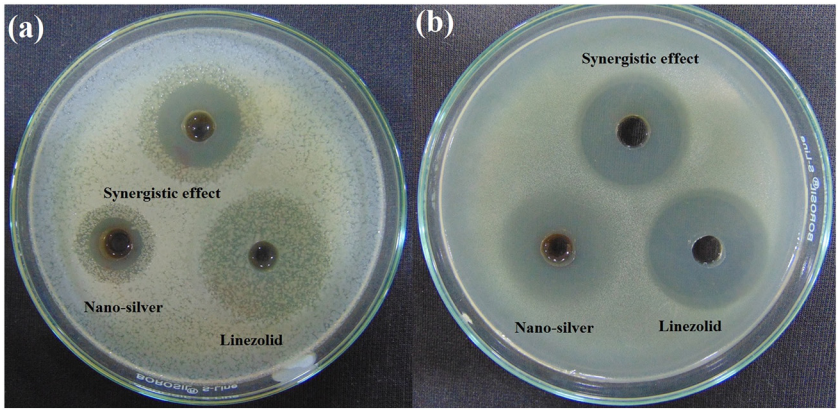

Fig. 7. Synergistic effect of linezolid with silver nanoparticles against (a). *E. coli* MTCC 443 and (b). *S. aureus* MTCC 3160.

Table 3
Bactericide activity of linezolid with and without nano-silver against Gram-negative *E. coli* MTCC 443 and Gram-positive *S. aureus* MTCC 3160 bacteria.

Bacterial strains	Zone of inhibition (mm)		
	Linezolid	Silver nanoparticles	Combination
E. coli MTCC 443	ND	6.00 ± 0.24	10.00 ± 0.18
S. aureus MTCC 3160	17.00 ± 0.10	16.00 ± 0.21	16.00 ± 0.16

ND: not detected. Values are expressed as mean ± SD for three independent experiments.

combinatorial option of nano-silver and antibiotics to combat Gram-negative bacteria regardless of their efflux-mediated resistance mechanism.

4. Conclusions

Linezolid is generally not active against Gram-negative organisms such as *E. coli* due to rapid efflux mechanisms, which reduces the cytoplasmic concentration of the linezolid to levels where it is ineffective. Hence, the present study focused on increasing the bactericide efficiency of linezolid against Gram-negative bacteria by using nano-silver. Nano-silver is one of the well-known bactericide substances, which act on bacterial surface. In the present study, that nano-silver synthesized from stem extract of *T. cordifolia* engaged in surface disruption, depressed the activity of membrane and encouraged their potential for increasing linezolid's bactericide efficiency. Notably, the strain of *E. coli* MTCC 443 was inhibited in the combinatorial assays to a much greater extent to when nano-silver and linezolid were used in isolation; suggesting that linezolid can be used in combination with nano-silver in order improve their bactericidal efficiency against Gram-negative bacteria. Furthermore, the synergistic bactericide activity of green synthesized nano-silver with linezolid can be reduced the need for high dosages and minimize cytotoxic effect. It is encouraging to note that the concentrations of nano-silver active against bacteria in synergic study have been shown lower (50 μg/mL) than the reference doses (200 μg/mL) for humans that can be chronically ingested [49]. Taken together, this is the first report documenting the effectiveness of linezolid against multidrug-resistant, Gram-negative pathogens with its possible mechanism. In the long term, more research in this direction might be lead to establishment of combination therapy of linezolid with nano-silver for multidrug-resistant, Gram-negative pathogens.

Funding

This research did not receive any specific grant from funding agencies in the public, commercial, or not-for-profit sectors.

Declaration of Competing Interest

The authors declare that they alone are responsible for the writing and content of this paper. The authors report no conflicts of interest in this research work.

Acknowledgments

The authors convey their thanks to Department of Biotechnology, Junagadh Agricultural University, Junagadh, Gujarat, India, for providing lab facilities to conduct the research work and analysis with SEM-EDX and GC–MS for fulfilment of the research work. This research did not receive any specific grant from funding agencies in the public, commercial, or not-for-profit sectors.

Appendix A. Supplementary data

Supplementary data to this article can be found online at https://doi.org/10.1016/j.lfs.2019.05.072.

References

[1] R.J. Fair, Y. Tor, Antibiotics and bacterial resistance in the 21th century, Perspectives in Medicinal Chemistry, vol. 6, 2014, pp. 25–64.
[2] M. Aikaterini, K. Konstantiana, I. Ioannis, Multi-drug resistant gram negative pathogens in long term care facilities: a steadily arising problem, J Infect Dis Diagn 1 (2015) 101.
[3] S. Vasoo, J.N. Barreto, P.K. Tosh, Emerging issues in Gram-negative bacterial resistance: an update for the practicing clinician, Mayo Clin. Proc. 3 (2015) 395–403.
[4] L. Chen, R. Todd, J. Kiehlbauch, M. Walters, A. Kallen, Pan-resistant New Delhi metallo-beta- lactamase-producing *Klebsiella pneumoniae* — Washoe County, Nevada, 2016, Morb. Mortal. Wkly Rep. 66 (2017) 33.
[5] E. Peterson, P. Kaur, Antibiotic resistance mechanisms in bacteria: relationships between resistance determinants of antibiotic producers, environmental bacteria, and clinical pathogens, Front. Microbiol. 9 (2018) 2928.
[6] X.Z. Li, P. Plesiat, H. Nikaido, The challenge of efflux-mediated antibiotic resistance in Gram-negative bacteria, Clin. Microbiol. Rev. 28 (2015) 337–418.
[7] H. Nikaido, J.M. Pages, Broad-specificity efflux pumps and their role in multidrug resistance of Gram-negative bacteria, FEMS Microbiol. Rev. 36 (2012) 40–63.
[8] I. Jung, E.J. Joo, B.S. Suh, C.B. Ham, J.M. Han, Y.G. Kim, J.S. Yeom, J.Y. Choi, J.H. Park, A case of generalized argyria presenting with muscle weakness, Annals of Occupational and Environmental Medicine 29 (2017) 45.
[9] H.T. Ratte, Bioaccumulation and toxicity of silver compounds: a review, Environ. Toxicol. Chem. 18 (1999) 89–108.
[10] T. Monowar, M.S. Rahman, S.J. Bhore, G. Raju, K.V. Sathasivam, Silver nanoparticles synthesized by using the endophytic bacterium *Pantoea ananatis* are promising antimicrobial agents against multidrug resistant bacteria, Molecules 23 (2018) 3220.
[11] R. Salomoni, P. Leo, A.F. Montemor, B.G. Rinaldi, M.F.A. Rodriques, Antibacterial effect of silver nanoparticles in *Pseudomonas aeruginosa*, Nanotechnol. Sci. Appl. 10 (2017) 115–121.
[12] C.H.N. Barros, S. Fulaz, D. Stanisic, L. Tasic, Biogenic Nanosilver against multidrug-resistant bacteria (MDRB), Antibiotics 7 (2018) 69.
[13] S.A. Anuj, H.P. Gajera, D.G. Hirpara, B.A. Golakiya, Bactericidal assessment of nano-silver on emerging and re-emerging human pathogens, J. Trace Elem. Med. Biol. 51 (2019) 219–225.

[14] M.S. Dryden, Linezolid pharmacokinetics and pharmacodynamics in clinical treatment, J. Antimicrob. Chemother. 66 (2011) iv7–iv15.
[15] N. Pandit, R.K. Singla, B. Shrivastava, Current updates on oxazolidinone and its significance, Int. J. Med. Chem. 2012 (2012) 15928.
[16] K. Takrouri, H.D. Cooper, A. Spaulding, P. Zucchi, B. Koleva, D.C. Cleary, W. Tear, P.J. Beuning, E.B. Hirsch, J.B. Aggen, Progress against *Escherichia coli* with the oxazolidinone class of antibacterials: test case for a general approach to improving whole-cell gram-negative activity, ACS Infectious Diseases 2 (2016) 405–426.
[17] P. Mukeshwar, K. Surendra, K. Manoj, S. Rohit, S. Gulab, P. Bisen, *Tinospora cordifolia*: a climbing shrub in health care management, Int. J. Pharm. Bio Sci. 3 (2012) 612–628.
[18] I. Mohammed, I. Mohd, K. Shaista, Bactericide activity of *Syzigium cumini* leaf extracts against multidrug resistant pathogenic bacteria, Journal of Applied Pharmaceutical Science 7 (2017) 168–174.
[19] R. Veluchamy, K. Chandran, R. Ayyappan, Evaluation of synergistic and bactericide activity of Xylaria curta against drug-resistant *Staphylococcus aureus* and *Pseudomonas aeruginosa*, Mycology 3 (2012) 252–257.
[20] S.A. Anuj, H.P. Gajera, D.G. Hirpara, B.A. Golakiya, Interruption in membrane permeability of drug-resistant *Staphylococcus aureus* with cationic particles of nano-silver, Eur. J. Pharm. Sci. 127 (2019) 208–216.
[21] M. Kuhn, D. Szklarczyk, S. Pletscher-Frankild, T. Blicher, C. Mering, L. Jensen, P. Bork, STITCH 4: integration of protein–chemical interactions with user data, Nucleic Acids Res. 42 (2013) D401–D407.
[22] D. Szklarczyk, A. Santos, C. Mering, L. Jensen, P. Bork, M. Kuhn, STITCH 5: augmenting protein–chemical interaction networks with tissue and affinity data, Nucxleic Acids Research 44 (2016) D380–D384.
[23] M. Kuhn, D. Szklarczyk, A. Franceschini, C. Mering, L. Jensen, P. Bork, STITCH 3: zooming in on protein-chemical interactions, Nucleic Acids Res. 40 (2012) D876–D880.
[24] G. Kanehisa, KEGG: Kyoto encyclopedia of genes and genomes, Nucleic Acids Res. 28 (2000) 27–30.
[25] M. Ashburner, C.A. Ball, J.A. Blake, D. Botstein, H. Butler, J.M. Cherry, A.P. Davis, K. Dolinski, S.S. Dwight, J.T. Eppig, M.A. Harris, D.P. Hill, L. Issel-Tarver, A. Kasarskis, S. Lewis, J.C. Matese, J.E. Richardson, M. Ringwald, G.M. Rubin, G. Sherlock, Gene ontology: tool for the unification of biology, The Gene Ontology Consortium Nat Genet 25 (2000) 25–29.
[26] M.R. Yen, J. Choi, M.H. Saier, Bioinformatic analyses of transmembrane transport: novel software for deducing protein phylogeny, topology, and evolution, J. Mol. Microbiol. Biotechnol. 17 (2009) 163–176.
[27] H. Suman, K. Kirendra, S. Ratul, M. Sudipta, S. Pritam, H. Saubhik, K. Sanmoy, S. Tuhinadri, Alteration of Zeta potential and membrane permeability in bacteria: a study with cationic agents, SpringerPlus 4 (2015) 672.
[28] L. Wen-Ru, X. Xiao-Bao, S. Qing-Shan, Z. Hai-Yan, O. You-Sheng, C. Yi-Ben, Bactericide activity and mechanism of silver nanoparticles on *Escherichia coli*, Appl. Microbiol. Biotechnol. 85 (2010) 1115–1122.
[29] R.C. Torane, G.S. Kamble, T.V. Gadkari, S. Amruta, A.S. Tambe, R. Nirmala, N.R. Deshpande, GC–MS study of nutritious leaves of Ehretia laevis, Int. J. Chem. Technol. Res. 3 (2011) 1589–1591.
[30] K. Januszek, E. Blonska, J. Dluga, J. Socha, Dehydrogenase activity of forest soils depends on the assay used, International Agrophysics 29 (2015) 47–59.
[31] M. Chen, Z. Yang, H. Wu, X. Pan, X. Xie, C. Wu, Antimicrobial activity and the mechanism of silver nanoparticle thermosensitive gel, Int. J. Nanomedicine 6 (2011) 2873–2877.
[32] A.K. Suresh, M.J. Doktycz, W. Wang, J.W. Moon, B. Gu, H.M. Meyer, D.K. Hensley, D.P. Allison, T.J. Phelps, D.A. Pelletier, Monodispersed biocompatible silver sulfide nanoparticles: facile extracellular biosynthesis using the c-proteobacterium, Shewanella oneidensis, Acta Biomater. 7 (2011) 4253–4258.
[33] J.A. Delmar, Su Chih-Chia, E.W. Yu, Bacterial multi-drug efflux transporters, Annu. Rev. Biophys. 43 (2014) 93–117.
[34] N.L. Brown, J.V. Stoyanov, S.P. Kidd, J.L. Hobman, The MerR family of transcriptional regulators, FEMS Microbiol. Rev. 27 (2003) 145–163.
[35] P. Rietveld, L.D. Arscott, A. Berry, N.S. Scrutton, M.P. Deonarain, R.N. Perham, C.H. Williams, Reductive and oxidative half-reactions of glutathione reductase from *Escherichia coli*, Biochemistry 33 (1994) 13888–13895.
[36] D.M. Clarke, P.D. Bragg, Purification and properties of reconstitutively active nicotinamide nucleotide transhydrogenase of *Escherichia coli*, Eur. J. Biochem. 149 (1985) 517–523.
[37] R. Darshan, P. Kirti, Bactericidal potential of silver nanoparticles synthesized using cell-free extract of *Comamonas acidovorans*: in vitro and in silico approaches, 3 Biotech 7 (2017) 92.
[38] S.L. Katherine, V. Birte, Resistance to linezolid caused by modifications at its binding site on the ribosome, Antimicrob. Agents Chemother. 56 (2012) 603–612.
[39] E.C. Hobbs, X. Yin, B.J. Paul, J.L. Astarita, G. Storz, Conserved small protein associates with the multidrug efflux pump AcrB and differentially affects antibiotic resistance, Proc. Natl. Acad. Sci. U. S. A. 109 (2012) 16696–16701.
[40] M. Arakha, M. Saleem, C. Bairagi, J. Mallick Suman, The effects of interfacial potential on antimicrobial propensity of ZnO nanoparticle, Sci. Rep. 5 (2015) 9578.
[41] M.E. Falagas, S.K. Kasiakou, Colistin: the revival of polymyxins for the management of multidrug-resistant Gram-negative bacterial infections, Clin. Infect. Dis. 40 (2005) 1333–1341.
[42] D. Balaram, D. Sandeep, M. Debasis, A. Jaydeep, C. Sourav, T. Satyajit, D. Aditi, M. Subhankar, D. Sankar, D. Debasis, R. Somenath, Green synthesized silver nanoparticles destroy multidrug resistant bacteria via reactive oxygen species mediated membrane damage, Arab. J. Chem. 10 (2017) 862–876.
[43] R. Campilongo, M.L. Di Martino, L. Marcocci, P. Pietrangeli, A. Leuzzi, Molecular and functional profiling of the polyamine content in enteroinvasive *E. coli*: looking into the gap between commensal *E. coli* and harmful *Shigella*, PLoS One 9 (2014) e106589.
[44] H.M. Shahjee, K. Banerjee, F. Ahmad, Comparative analysis of naturally occurring L-amino acid osmolytes and their D-isomers on protection of *Escherichia coli* against environmental stresses, J. Biosci. 27 (2002) 515–520.
[45] S. Kim, L. Hyeong-Seon, R. Deok-Seon, C. Soo-Jae, L. Dong-Seok, Bactericide activity of silver-nanoparticles against *Staphylococcus aureus* and *Escherichia coli*, Korean J. Microbiol. Biotechnol. 39 (2011) 77–85.
[46] K. Boeneman, E. Crooke, Chromosomal replication and the cell membrane, Curr. Opin. Microbiol. 8 (2005) 143–148.
[47] D. Gupta, A. Singh, A.U. Khan, Nanoparticles as efflux pump and biofilm inhibitor to rejuvenate bactericidal effect of conventional antibiotics, Nanoscale Res. Lett. 12 (2017) 454.
[48] I. Ghai, S. Ghai, Understanding antibiotic resistance via outer membrane permeability, Infection and Drug Resistance 11 (2018) 523–530.
[49] Xi-Feng Zhang, Wei Shen, Sangiliyandi Gurunathan, Silver nanoparticle-mediated cellular responses in various cell lines: an in vitro model, Int. J. Mol. Sci. 17 (2016) 1603.